

## **Ion Transport Simulation Using Geant4 Hadronic Physics**

**T. Koi**

SLAC

Menlo Park, CA 94025, USA

[tkoi@SLAC.stanford.edu](mailto:tkoi@SLAC.stanford.edu)

**G. Folger, B. Trieu, and J. P. Wellisch**

CERN

Geneva, Switzerland

**I. Corneliu**

INFN

Torino, Italy

**P. Truscott**

QinetiQ

Farnborough, UK

### **ABSTRACT**

We discuss the recently developed capability of Geant4 to simulate ion transport. This development includes two main functionalities: cross section calculations and final state generation for a set of ion-ion interactions. For the cross section calculation, several empirical cross section formulae for the total reaction cross section of ion-ion interactions were implemented. For the final state generators, the binary cascade and quark-gluon string models of Geant4 were improved so that ion reactions with matter may also be calculated.

*Key Words:* Monte Carlo, ion-ion interaction

### **1 INTRODUCTION**

The transportation of ions in matter is a subject of much interest, not only in high-energy ion-ion collider experiments such as RHIC and LHC, but also in many other fields of science, engineering and medical applications.

Hence, we have added ion transport capabilities to Geant4 [1]. Geant4 is a toolkit for the simulation of the passage of particles through matter, and was created by exploiting software engineering and object-oriented technology. The hadronic interaction framework within Geant4 [2] was also designed with this technology. The implementation of the framework follows the Russian dolls (Матрёшка) approach to object-oriented design, resulting in a multi-layer hierarchy.

In this paper we first briefly discuss the hadronic interaction framework in Geant4, especially its second-level framework (cross sections and models). Implemented cross sections and models for ion interactions are then described and several validation plots will be shown. We also briefly

refer to other ion-related processes implemented in Geant4. Finally we summarize the current status of ion transport simulation using Geant4 hadronic physics.

## 2 GEANT4 HADRONIC INTERACTION FRAMEWORKS

The hadronic interaction framework in Geant4 consists of a multi-layer hierarchy. The top level of the framework provides the basic interface to the other Geant4 categories, such as tracking. As the hierarchy is descended, lower framework levels refine the interfaces for increasingly more specific use cases. Each level under the top has a concrete implementation of the abstract interface from the framework level directory above it, encapsulating the common logic. In this paper, only the second-level framework (cross sections and models) is discussed. A detailed description of the entire framework is given by J. P. Wellisch [2]. Fig. 1 is a schematic view of the relevant part of the second-level framework. At this level there are two important concepts: cross sections and models. The simulation must acquire two pieces of information from a specific interaction: where and when it will occur, and what will happen due to the interaction. The former is determined by cross sections and the later is calculated by models. In this framework, the word "model" means the final state generator. The cross sections and models which were developed for this work are explained below.

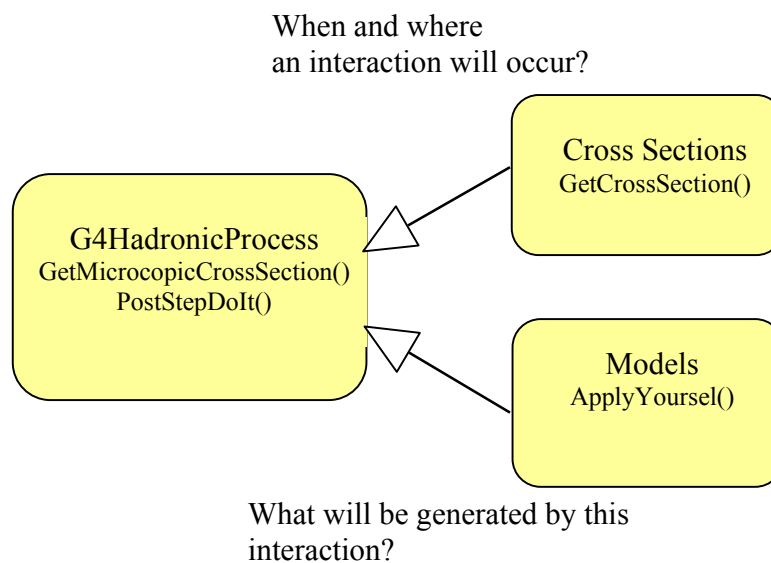


**Figure 1, Schematic view of the second level framework of hadronic interactions in Geant4.**

## 3 CROSS SECTIONS

The total reaction cross section,  $\sigma_R$ , is given by

$$\sigma_R = \sigma_{Tot} - \sigma_{El} - \sigma_{EMdis} \quad (1),$$

where  $\sigma_{Tot}$  is the total cross section,  $\sigma_{El}$  is the elastic cross section and  $\sigma_{EMdis}$  is the electromagnetic dissociation cross section. It has been widely studied both theoretically and experimentally

Several empirical formulae have been developed for the calculation of the total reaction cross sections of nucleus-nucleus collisions since the first proposal by Bradt and Peters [3] which was presented more than a half-century ago. In order to cover all combinations of colliding nuclei over a wide energy range, the cross section formulae of Tripathi [4, 5], Shen [6], Kox [7] and Sihver [8] were implemented in Geant4. These are empirical and parameterized formulae which include theoretical aspects such as Coulomb barrier, Pauli blocking, asymmetric proton and neutron numbers and so on. The basic form of these formulae are similar to each other, such as

$$\sigma_R = \pi r_0^2 (R_{vol} + R_{surf})^2 \left(1 - \frac{B_C}{E_{C.M.}}\right), \quad (2)$$

where  $r_0$  is a constant related to the radius of the nucleon.  $R_{vol}$  and  $R_{surf}$  correspond to the energy-independent and energy-dependent components of the reactions, respectively. The former is given by the mass number of projectile and target nuclei ( $A_p$  and  $A_t$ ).

$$R_{vol} = \left( A_p^{\frac{1}{3}} + A_t^{\frac{1}{3}} \right), \quad (3)$$

and represents the volume component of the reactions. The later stands for nuclear surface contributions including the mass asymmetry of projectile and target nuclei, nuclear transparency effect which depends on the projectile energy and so on. The last term is the Coulomb interaction term.  $B_c$  is the Coulomb barrier of the projectile-target system and  $E_{C.M.}$  is the center-of-mass energy of the colliding system. The values of  $r_0$  and detailed derivation methods of  $R_{surf}$  and  $B_c$  differ for each formula. Fig. 2 shows the calculated result of each formula for the collision of two  $^{12}\text{C}$  nuclei, together with some experimental data [7, 9] and theoretically calculated values from the microscopic model [10].

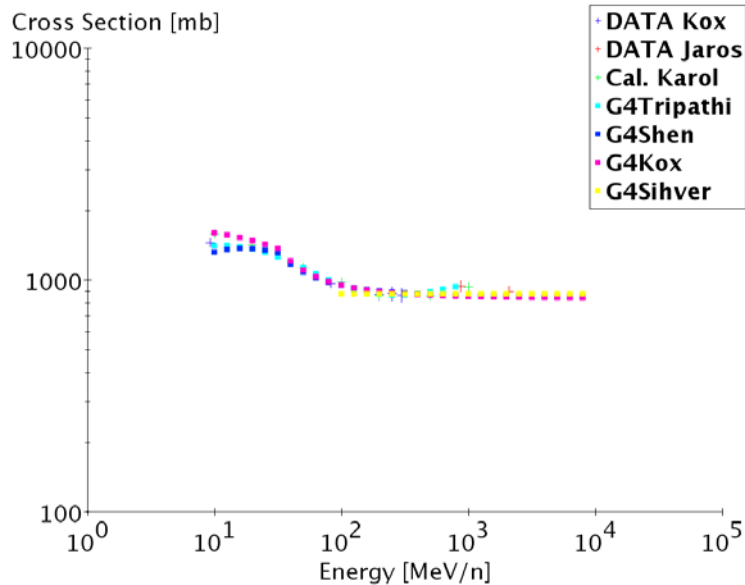


**Figure 2. Comparison of total reaction cross sections of collisions between  $^{12}\text{C}$  and  $^{12}\text{C}$ .**

Since there are many cross section formulae for nucleus-nucleus collisions in Geant4, the class `G4GeneralSpaceNNCrossSection` was prepared to assist users in selecting the appropriate cross section formula.

## 4 MODELS

We improved the Binary Cascade model [11] and the Quark Gluon String (QGS) model of Geant4 so that ion reactions with matter can be calculated. In this section we briefly explain both models together with points of improvement in the final state generators of ion interactions.

### 4.1 Binary Cascade Light Ion

The Binary Cascade model is based on a detailed three-dimensional model of the nucleus, and exclusively based on binary scattering between reaction participants and nucleons within this nuclear model. This feature makes it a hybrid between a classical cascade code, and a quantum molecular dynamic (QMD) model. In the Binary Cascade model, similar to QMD, each participating nucleon is seen as a Gaussian wave packet and the total wave function is assumed to be the direct product of the wave functions of the participating particles without anti-symmetrization. Here, participating means that they are either primary particles, or have been generated or scattered in the process of cascade.

The resulting equations of motion have the same structure as the classical Hamilton equations and can be solved numerically. However, unlike the QMD model where the Hamiltonian is self-generated from the system configuration, the Hamiltonian is calculated using simple time-independent optical potentials. A three-dimensional nuclear model is constructed from the atomic number and the mass number. The nucleon distribution follows the Woods-Saxon model [12] for heavy nuclei and the harmonic oscillator shell model [13] for light nuclei which have mass numbers smaller than 17. Nucleon momenta are sampled from 0 up to the Fermi momentum and the sum of these momenta is set to 0. The time-invariant scalar optical potentials are used for the nuclear field effects. The time integration of the reactions is carried out as follows. First the impact parameter is sampled and the time to closest approach of the projectile to the nucleons in the nucleus is calculated. In this calculation the momentum of the target nucleons is ignored. The reactions are selected according to the free hadron-nucleon cross section. For the calculation of the cross-section, the momenta of the nucleons are taken into account. Transportation of the system to the time of the first collision or decay is advanced. New products are created while taking the Pauli exclusion principle into account. This procedure is repeated for all products, hence allowing for re-scattering. The cascade terminates when the average energy of all participants within the nucleus are below a given threshold; then the residual participants and the nucleus in that state will be treated by pre-equilibrium decay.

In nucleus-nucleus interactions, two nuclei are prepared according to this three-dimensional nuclear model. The lighter nucleus is selected to be the projectile. Nucleons in the projectile are entered with position and momenta into the initial collision state. Until the first collision of each nucleon of the projectile, its Fermi motion is neglected in tracking. Fermi motion and the nuclear field are taken into account in collision probabilities and final states of the collisions. The nucleon distribution inside the projectile nucleus is taken to be a representative distribution of its nucleons in configuration space, rather than an initial state in the sense of QMD. Projectile

excitation energy is determined from the binary collision participants (P) using the statistical approach towards excitation energy calculation in an adiabatic abrasion process [14]

$$E_{ex} = \sum_P (E_{fermi}^P - E^P). \quad (4)$$

Given this excitation energy, the projectile fragment is then treated by the pre-equilibrium decay.

## 4.2 QGS-Glauber

In Geant4, parton string models are used to generate the final state inelastic interactions of hadrons with nuclei at high incident energies. Such models can be divided into two phases: string excitation and string fragmentation. Two models which have different approaches to the string excitation phase are implemented. One is based on diffractive excitation and the other (QGS model) is based on soft scattering with diffractive admixture according to cross sections. In the string fragmentation phase, two models have basically common treatments, using different fragmentation functions. In hadron-nucleus reactions in the QGS model, a three-dimensional nucleus is built up in a manner similar to that of the Binary Cascade model and then collapsed to two dimensions. The impact parameter is sampled and then the hadron-nucleon collision probabilities are calculated based on the quasi-eikonal model. The number of Pomerons which are exchanged in each collision is sampled. String formation is done via parton exchange and the rearrangement mechanism. Produced strings enter into the string fragmentation phase so that secondary white hadrons are produced by string fragmentation. This fragmentation of a string follows an iterative scheme where a string produces a hadron and new string. The LUND model [15] fragmentation function is implemented and used not only for fragmentation but also for the decay of the excited string. In order to achieve better three-reggeon behavior when the light cone momentum fraction is close to 1, the special fragmentation functions [16] of the QGS model are also implemented. Hadron formation points from string fragmentation are assumed to be given by the yo-yo formation point.

The QGS model treats a hadron-nucleus collision as a set of quasi-independent hadron-nucleon collisions, correlated only through quark-content and energy conservation. In nucleus-nucleus reactions, according to the nucleus model of the projectile ion, the additional primary nucleons are put into the reaction system. We have developed this feature but it has not yet been included in the latest release of Geant4 (version 6 with patch 02).

## 5 VALIDATION WITH EXPERIMENTS

A validation suite has been developed to evaluate and optimize hadronic models in Geant4. We have performed several validations by comparing simulation results with experimental data, samples of which are shown in Figs. 3, 4, 5 and 6. Fig. 3 shows the double differential cross sections for negative pion production by a  $^{12}\text{C}$  beam at 1.05 (GeV/c)/n. The emission angle of secondary pions is 2.5 degrees and each plot corresponds to a different target material, beryllium, carbon, copper and lead.

Iwata et al. [17] measured the double differential cross sections for neutron production from C, Ne, and Ar projectiles at 290–600 MeV/n on C, Cu, and Pb targets. We compared their measurements and Geant4 simulation. One of the results, shown in Fig. 4, is the double

differential neutron production cross section for a  $^{12}\text{C}$  beam at 290 MeV/n bombarding a copper target. Each plot corresponds to a different emission angle of secondary neutrons. The measured neutron spectra were compared with those calculated by the QMD code [18] and HIC code [19] by the original authors. To make a quantitative comparison between the measured and calculated cross sections, they defined the ratio  $R$  as

$$R = \frac{\left(\frac{d\sigma}{d\Omega}\right)_m - \left(\frac{d\sigma}{d\Omega}\right)_c}{\left(\frac{d\sigma}{d\Omega}\right)_m}, \quad (5)$$

where  $m$  and  $c$  refer to the measured and calculated  $d\sigma/d\Omega$  respectively. We also calculate the ratios  $R$  with the Geant4 simulation. However, in the numerator we subtract calculated from measured values instead of measured from calculated values as done by the original authors. The values of  $R$  are plotted in the Fig. 5 as a function of laboratory angle. The error bars on the plot are estimated from experimental errors which include both systematic and statistical uncertainties, because the statistical uncertainties of the Monte Carlo simulation are small enough to be neglected. Except for the carbon projectiles at 400 MeV/n where over-estimation of neutron production is seen, there is no systematic correlation between the projectiles and the targets. The ratios of carbon projectiles are spread more broadly than other, heavier projectiles. This tendency is also seen in Fig. 12 and 13 of Iwata et al. and compared with the distribution of  $R$ s in the figures, agreements with Geant4 simulations are at least at the same level as their QMD and HIC calculations. Even though they concluded rather severely that neither QMD nor HIC could reproduce the measured cross sections for all combinations of the projectiles and targets, we think the result is comfortable, considering that model development is in its early stages. As mentioned before, the Binary Cascade Light Ion model will exchange a projectile nucleus and a target nucleus, when the projectile is heavier than the target. Ne and Ar projectiles on carbon targets are examples. In Fig5, no significant difference can be seen in the distributions of  $R$ s for C, Ne and Ar projectiles on heavier targets such as copper or lead, so that the swapping supposition seems to have succeeded. And it is also mentioned before that, unlike the QMD models, the Binary Cascade model does not treat collisions between participants. Once the number of participants increases and collisions between them become important, the limit of the model's application is approaching. This is more important for nucleus- nucleus collisions, since the number of participants starts from the mass number of the projectile nucleus. Because Ar has the largest mass number of the three projectiles we were interested in the  $R$  distributions of Ar projectiles on copper and lead targets, since a projectile swap has occurred with the carbon target. The agreements of these combinations of projectile and target are the same level as Ne which has a mass number of 20. Hence we consider that the application limit of the model will not be reached until Ar projectiles are used.

We also compared Geant4 simulations to neutron yields from bombarding ions on thick targets measured by Kurosawa et al. [20]. The thickness of each target corresponded to the stopping lengths of each primary ion. Fig. 6 is one of the results and shows double differential neutron yield for a  $^{56}\text{Fe}$  beam at 400MeV/n bombarding a thick copper target which has a thickness of 15mm. Even when a projectile has a mass number of 56, agreement is not so bad except in the forward direction. In the forward direction, the simulation greatly under-estimated the measurement. This tendency is observed in all combinations of projectile and target.

Validation work is continuing for many aspects of nucleus-nucleus reactions, including charge exchange cross sections and projectile fragmented particle production.

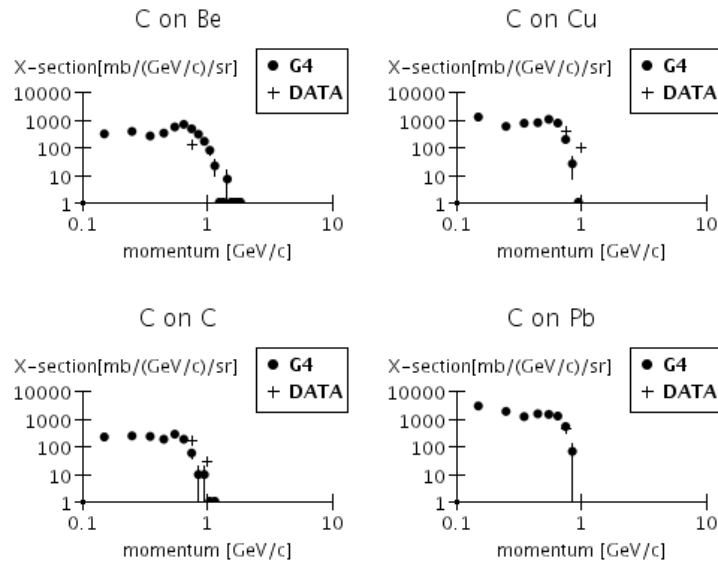


**Figure 3. Comparison of double differential (2.5 deg.) negative pion production cross sections for a C beam of 1.05 (GeV/c)/n between data [21] and Geant4 simulation. Target materials are Beryllium, Carbon, Copper and Lead.**

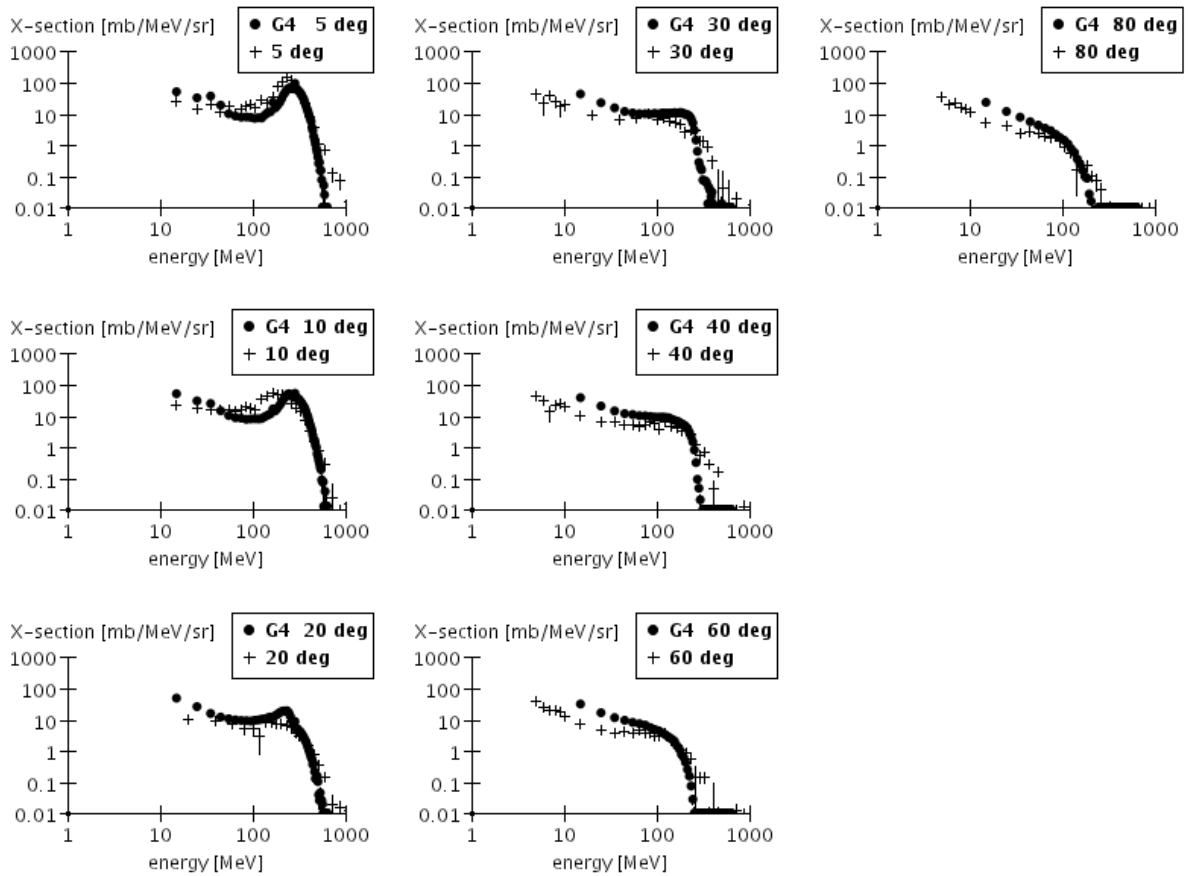


**Figure 4. Comparison of double differential neutron production cross sections for a C beam of 290 MeV/n on Copper between data [17] and Geant4 simulation.**

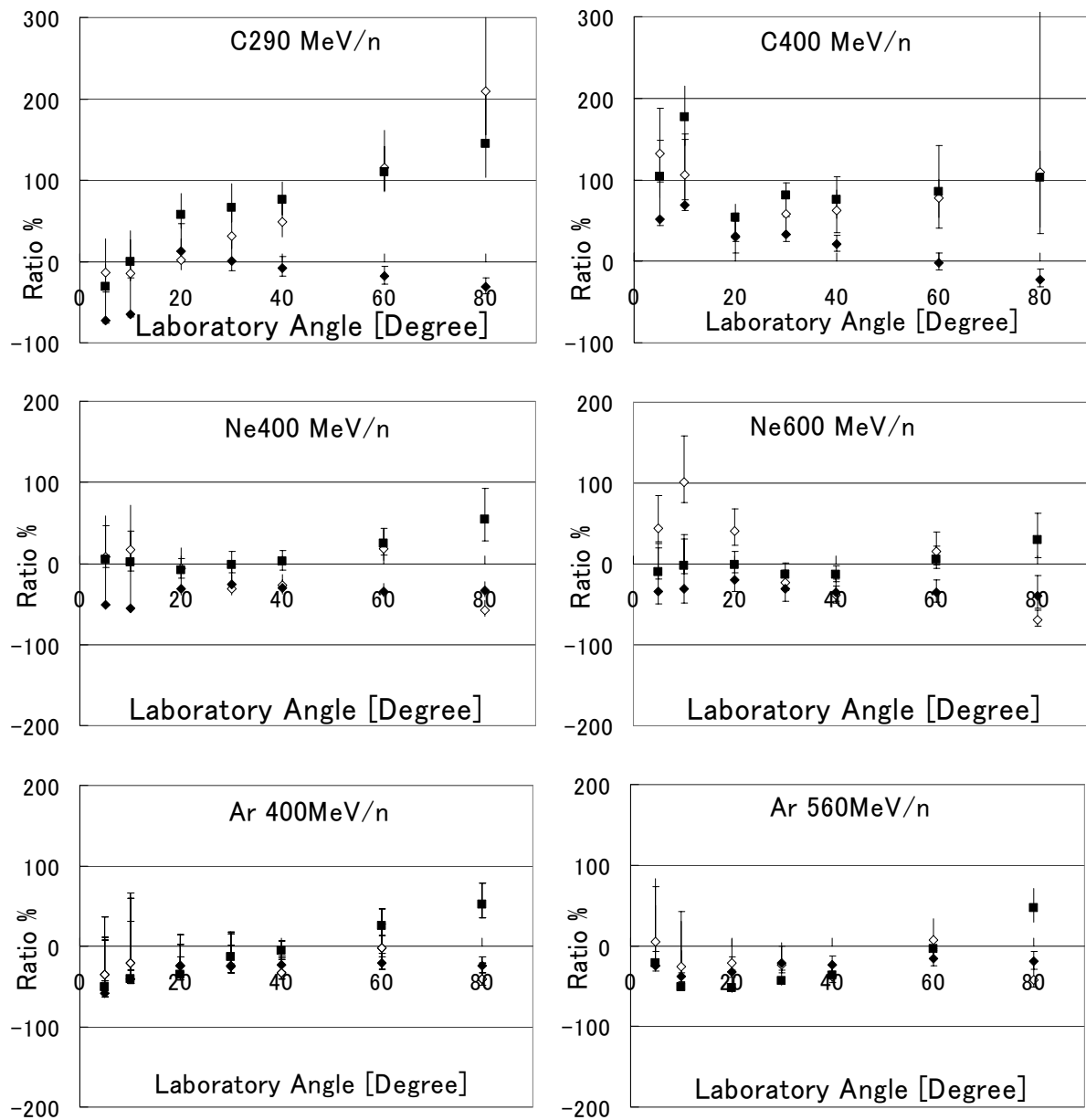


**Figure 5. Ratios R calculated by Geant4 simulation. The species and energy of projectiles are written in each plot and the open diamonds, filled circles, and filled diamonds, show the ratios for the C, Cu, and Pb targets, respectively.**

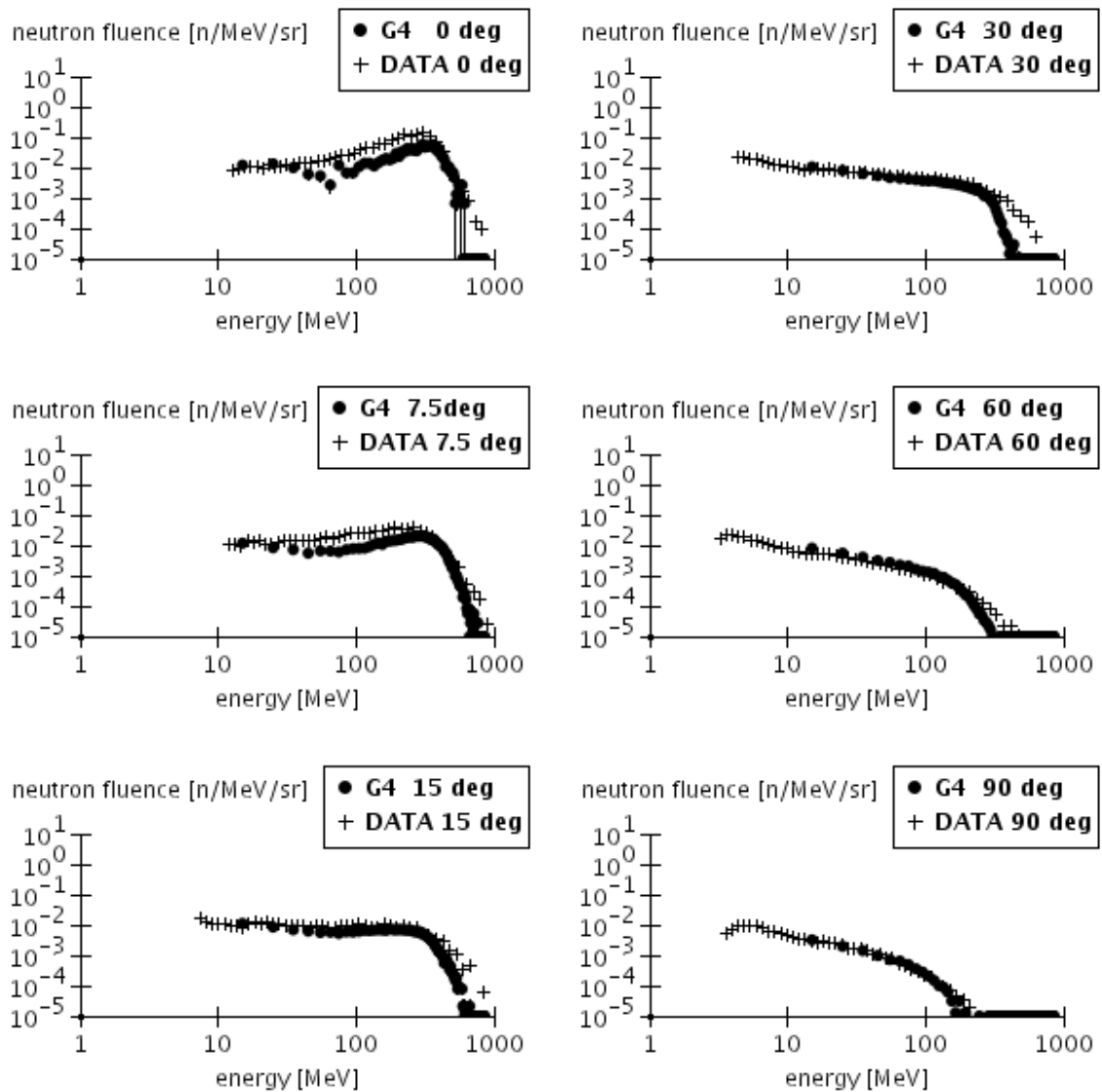


**Figure 6. Comparison of double differential neutron production for a Fe beam of 400 MeV/n on a thick Copper target (1.5cm) between data [20] and Geant4 simulation.**

## 6 OTHER ION RELATED PROCESSES IN GEANT4

Geant4 already has many other ion-related processes such as,

- Ionization Energy Loss
- Multiple Coulomb Scattering
- Electromagnetic Dissociation
- Abrasion-Ablation Model

Electromagnetic dissociation is the interaction between the projectile particle and virtual photons which appear when relativistic projectiles pass the target nucleus. The cross section of this process becomes especially important when projectile energies are ultra-relativistic and the atomic number of the nucleus is large.

The Abrasion-Ablation Model is a simplified macroscopic model for nuclear-nuclear interactions based largely on geometric arguments rather than a detailed consideration of nucleon-nucleon collisions. The computing speed of this model is faster than microscopic models such as the Binary Cascade and QGS-Glauber, making it a useful alternative.

A detailed description of electromagnetic dissociation and the abrasion-ablation model in Geant4 is given by Truscot et al.[22].

All of the above processes are integrated into ion transportation in Geant4.

## 7 CONCLUSIONS

We have developed functionalities for ion transport simulation in Geant4. Within the hadronic interaction framework of Geant4, cross sections for nucleus-nucleus reactions have been added and the Binary Cascade and QGS models have been extended to handle ion interactions.

Fig. 7 shows that there is no significant gap the area covered by both cross sections and models for nucleus-nucleus interactions. Geant4 now has abundant processes for ion interactions with matter and without any extra modules, users may simulate ion transportation using the complex and realistic geometries of Geant4. Validation has begun and the first results show reasonable agreement with data. This work continues.

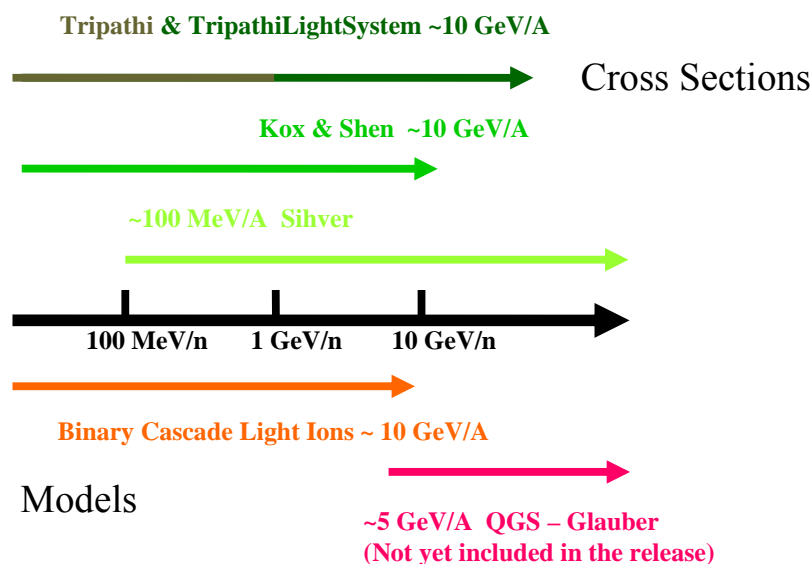


Figure 7. Area covered by models and cross sections for ion interactions.

## 8 ACKNOWLEDGEMENTS

The authors would like to express thanks to Dr. D. H. Wright for careful reading the manuscript. The work of T. K. was supported by Department of Energy contract DE-AC03-76SF00515.

## 9 REFERENCES

- [1] GEANT4 Collaboration S. Agostinalli et al., “Geant4—a simulation toolkit” *Nucl. Instr. Meth.* **A506** pp. 250-303 (2003).  
<http://geant4.web.cern.ch/geant4/>
- [2] J. P. Wellisch, “Hadronic shower models in Geant4 — the frameworks,” *Comp. Phys. Commun.* **140** pp.65-75 (2001).
- [3] H. L. Bradt and B. Peters, “The Heavy Nuclei of the Primary Cosmic Radiation,” *Phys. Rev.* **77** pp.54-70 (1950)
- [4] R. K. Tripathi, F. A. Cucinotta and J. W. Wilson, “Universal Parameterization of Absorption Cross Sections,” NASA Technical Paper TP-3621 (1997).
- [5] R. K. Tripathi, F. A. Cucinotta and J. W. Wilson, “Universal Parameterization of Absorption Cross Sections -Light Systems-,” NASA Technical Paper TP-209726 (1999).
- [6] S. Kox et al., “Trends of total reaction cross sections for heavy ion collisions in the intermediate energy range,” *Phys. Rev.* **C35** pp.1678-1691 (1987).
- [7] Wen-qing Shen et al., “Total reaction cross section for heavy-ion collisions and its relation to the neutron excess degree of freedom,” *Nucl. Phys.* **A491** pp.130-146 (1989).
- [8] L. Sihver et al., “Total reaction and partial cross section calculations in proton-nucleus ( $Z_t \leq 26$ ) and nucleus-nucleus reactions ( $Z_p$  and  $Z_t \leq 26$ ),” *Phys. Rev.* **C47** pp. 1225-1236 (1993).
- [9] J. Jaros et al., “Nucleus-nucleus total cross sections for light nuclei at 1.55 and 2.89 GeV/c per nucleon,” *Phys. Rev.* **C18** pp. 2273-2292 (1978).
- [10] P. J. Karol, “Nucleus-nucleus reaction cross sections at high energies: Soft-spheres model,” *Phys. Rev.* **C11** pp. 1203-1209 (1975) and T. Brohm K. -H. Schmidt, “Statistical abrasion of nucleons from realistic nuclear-matter distributions,” *Nucl. Phys.* **A569** pp. 821-832 (1994).
- [11] G. Folger, V. N. Ivanchenko and J. P. Wellisch, “The Binary Cascade - Nucleon nuclear reactions,” *Eur. Phys. J.* **A21** pp. 407-417 (2004).
- [12] M. E. Grypeos et al., “The 'cosh' or symmetrized Woods-Saxon nuclear potential,” *J. Phys.* **G17** pp. 1093-1105 (1991).
- [13] L. R. B. Elton, *Nuclear Sizes*, Oxford University Press, Oxford, (1961).
- [14] J. J. Gaimard and K. H. Schmidt “A Reexamination of the abrasion - ablation model for the description of the nuclear fragmentation reaction,” *Nucl. Phys.* **A531** pp. 709-745 (1991).
- [15] B. Andersson et al., “Parton fragmentation and string dynamics,” *Phys. Rep.* **97** pp. 31-145 (1983).

- [16] A. B. Kaidalov, "Quark And Diquark Fragmentation Functions In The Model Of Quark Gluon Strings" *Yad. Fiz.* **45** pp. 1452-1461 (*Sov. J. Nucl. Phys.* **45** pp. 902-907) (1987).
- [17] Y. Iwata et al., "Double-differential cross sections for the neutron production from heavy-ion reactions at energies  $E/A = 290\text{--}600$  MeV," *Phys. Rev. C* **64** pp. 05460901-05460910 (2001).
- [18] J. Aichelin, "'Quantum" molecular dynamics—a dynamical microscopic  $n$ -body approach to investigate fragment formation and the nuclear equation of state in heavy ion collisions" *Phys. Rep.* **202** pp. 233-360 (1991).
- [19] H.W. Bertini et al., "HIC-1: A First Approach to the Calculation of Heavy-Ion Reactions at Energies 50 MeV/Nucleon," Oak Ridge National Laboratory Report No. ORNL-TM-4134, (1974).
- [20] T. Kurosawa et al., "Neutron yields from thick C, Al, Cu, and Pb targets bombarded by 400 MeV/nucleon Ar, Fe, Xe and 800 MeV/nucleon Si ions," *Phys. Rev. C* **62** pp. 04461501-04461511 (2000)
- [21] J. Papp, thesis, University of California, Berkeley, Lawrence Berkeley Laboratory Report No. LBL-3633, (1975).
- [22] P. Truscot, et al. "Nuclear-Nuclear Physics in Geant4 for Interplanetary Space Missions," in Proceedings of the Monte Carlo 2005 Topical Meeting (2005).